Journal of Inorganic and Organometallic Polymers and Materials (2020) 30:808–819
https://doi.org/10.1007/s10904-019-01265-2

Calcium Iron Layered Double Hydroxide/Poly(vinyl chloride) Nanocomposites: Synthesis, Characterization and Cd^{2+} Removal Behavior

Mohammad Dinari[1] · **Negar Roghani**[1]

Received: 1 April 2019 / Accepted: 19 July 2019 / Published online: 24 July 2019

Abstract
Poly(vinyl chloride) (PVC) and other thermoplastics have received more attention in the last decades due to their high fire resistance, hydrophobicity, and flexibility. To improve the thermal stability of these classes of polymers, heat stabilizers should be used. Layered double hydroxides (LDHs) are a green and inexpensive class of heat stabilizers. In this study at first, the co-precipitation method was used to prepare nanostructure calcium/iron layered double hydroxide (Ca/Fe-LDH), and then it was organo-modified with citrate as a green and environmentally friendly anion. In the next step, it was used as a nanofiller for improving the thermal properties of the PVC matrix. Accordingly, LDH-Cit/PVC nanocomposites (NCs) with different amounts of LDH-Cit (5, 10 and 15 wt%) were synthesis by ultrasonic irradiation technique. The structural, morphological, and thermal properties of the synthesized NCs were evaluated with XRD, FT-IR, FE-SEM, TGA techniques. By introducing of LDH-Cit in the NCs, the residue at 800 °C was increased from 10 to 23% compared to pure PVC. The NCs ability to removing Cd^{2+} metal ion and the effects of time, pH, and Cd^{2+} concentration on the removal efficiency of Cd^{2+} were studied. Due to the increase of the adsorbent mass and removal efficiency of Cd^{2+}, the 60 mg L^{-1} of Cd^{2+} concentration and pH of 7 were chosen as the optimized condition. Also, kinetics studies on the experimental data for adsorbents showed acceptable adaptation with the Langmuir isotherm and pseudo-second-order kinetic model.

Keywords Layered double hydroxide · Surface modification · Poly(vinyl chloride) · Nanocomposite · Cd^{2+} removal · Isotherm

1 Introduction

One of the most important problems to human beings by the world population growth is demanding safe and non-toxic drinking water. However, currently, pollution is increasing by many natural and synthetic sources which results in contaminated water [1]. The most important and serious pollutants of water sources are heavy metals and halogen components, which are the reason for hazardous anions and oxyanions formation in water [2]. Serious health problems and diseases can cause the accumulation of these hazardous materials in the human body and other fellow creatures [3]. Cadmium ion is the most harmful and abundant pollutant among existing pollution sources of water based on heavy metal ions, which is generating extensive contamination in drinking water [4]. Therefore, the removal of cadmium ions from water and wastewater became a challenge from the viewpoints of green chemistry. Ion-exchange and adsorption methods are two simple techniques for elimination of heavy metallic ions from polluted water solution, which are chosen by most of the green chemists [5]. Recent studies on materials for elimination and removal of heavy metallic ions is introducing of organic compounds [6], inorganic materials [7] or materials with biologic source [8]. Nanostructure materials with large specific surface area and great surface activity are good candidates for adsorption of dangerous metal ions in polluted water solution [9].

Recently, peculiar and fascinating properties of layered silicate clays, calcium carbonate or silica nanoparticles [10, 11], have attracted increasingly growing interested to use them in reinforcing polymer nanocomposites (NCs) with the lower volume fraction of these materials [12, 13]. Ultra-large

✉ Mohammad Dinari
dinari@cc.iut.ac.ir; mdinary@gmail.com

[1] Department of Chemistry, Isfahan University of Technology, Isfahan 84156-83111, Islamic Republic of Iran

interfacial area per unit volume between nanofiller and a polymer matrix can only make by uniform dispersion of these nanofiller particles in polymer matrices [14, 15].

Poly(vinyl chloride) (PVC) is a polymer which is used in different cases such as profile applications like doors and windows, in making bottles, in non-food packaging, and bank or membership cards. However, a great disadvantage of PVC is its low thermal stability during the processing that leads to degradation. To overcome this problem, different heat stabilizers are being used. As a result, the industry needs a non-toxic and safe thermal stabilizer rather than compounds which are recently used in industry such as lead-based stabilizers, organo-tin compounds and mixed metal soaps for PVC [16, 17]. These nanomaterials which are characterized by the formula: $\left[M^{II}_{1-x}M^{III}_{x}(OH)_2\right](A^{m-})^{x/m} \cdot mH_2O$, where M^{II}, M^{III}, and A stand for divalent cation, trivalent cation, and the interlayer anion, respectively, are layered double hydroxides (LDHs) a series of 2D nanomaterials [15, 16]. The interlayer anion (A^{m-}) has been varied into a wide range and exchangeable capacity. High charge density of the LDH make it difficult to be exfoliate or delaminate when the LDHs being used as reinforcing fillers in polymer NCs. The selection of anions for the modification of LDH depends on the next application of the materials. Recent study show that LDHs containing interlayer carboxylate anions have significant consideration due to their potential applications to remove heavy metal ions from an aqueous solution [17]. Also, LDH having the capacity of absorbing HCl, it may be used as PVC thermal stabilizer. Previous studies show that different LDH based nanofiller were used as a heat stabilizer for PVC NCs [18–23].

In this investigation, first to achieve an effective functionalized material for removal of Cadmium ion from water, the synthesis of citrate intercalated calcium/iron layered double hydroxide (Ca/Fe-LDH) was selected. Then, the citrate modified LDH (LDH-Cit) as a potential thermal stabilizer was used as nanohybrid filler in the preparation of PVC NCs. Novel LDH-Cit/PVC NC films were synthesized by adding different amount of LDH-Cit nanoparticles (5, 10 and 15 wt%) through ultrasonic irradiation. The thermal and morphological properties of the LDH-Cit/PVC NC films have been investigated in details. Then, LDH-Cit/PVC NC was used for removing Cd^{2+} metal ion from aqueous solution. The adsorption kinetic and isotherm models were investigated.

2 Experimental

2.1 Chemicals

Iron (III) nitrate nine hydrate, calcium nitrate four hydrate, trisodium citrate and tetrahydrofuran (THF) were delivered from Merck chemical CO. Poly(vinyl chloride) (PVC) with Mw of 78,000 g mol^{-1} was used for the preparation of the NC. All the materials used without any further purification.

2.2 Synthesis of Ca/Fe LDH-Cit

Citrate modified Ca/Fe LDH was synthesized by using a modified homogeneous co-precipitation method as reported in our recently published paper [24].

2.3 Preparation of the LDH-Cit/PVC NC Films

In the first step, different mass percentages of LDH-Cit nanoparticle (5, 10 and 15 wt%) was suspended in 10 mL of THF and the mixture was ultrasonicated for 30 min. A solution of THF with 1.0 g of PVC was prepared at 50 °C and then the solution was added to the LDH-Cit suspension and refluxed for 1 h at the room temperature. Then LDH-Cit/PVC NC was irradiated with ultrasonic waves for 60 min. The resulting mixture was transferred into a glass tank and was dried at room temperature for 12 h. Finally, it was gradually dried at 50 °C in an oven for 3 h.

2.4 Characterization Techniques

A Bruker XRD which is equipped with a Cu Kα radiation in the range of $2\theta = 0.7°–80°$ at a scanning rate of 0.05° min^{-1} was used to record the X-ray diffraction (XRD) patterns. To study the functional groups of the LDH and NCs, FT-IR spectra (a Jasco-680 spectrometer) in the wavenumber range from 400 to 4000 cm^{-1} was employed. A Jasco V-570 UV–Vis spectrophotometer was used to investigate the optical properties of the NCs. Surface morphology of NCs was examined by a HITACHI S-4160 filed emission scanning electron microscope (FE-SEM). An STA503 TA was used to study the thermal stability of NCs from 30 to 800 °C at the rate of 10 °C min^{-1} under the argon atmosphere. A Testometric Universal Testing Machine M350/500 (UK) was employed for tensile testing at a speed of 5 mm min^{-1}. Samples were prepared with 40 mm by 10 mm with a thickness of 40 μm. At least three samples were tested for each type of samples. Sonication in the synthesis procedure was performed by using A SonoSwiss SW 3H ultrasonic bath (Ramsen, Switzerland) with the power of 280 W at 38 kHz. Flame atomic absorption spectrophotometer (FAAS; Perkin-Elmer 2380-Waltham) was used to determine the cadmium concentrations.

2.5 Adsorption Studies

The behavior of LDH-Cit/PVC NC 10 wt% and neat PVC for the removal of Cd^{2+} ions from solutions is studied by adsorption experiments under optimized condition.

The amount of cadmium adsorbed was calculated by Eq. (1):

$$Q_e = \frac{(Co - Ce)V}{m} \quad (1)$$

where Q_e (mg g^{-1}), C_0 and C_e (mg L^{-1}), V (L) and m (g) are cadmium adsorption value, the primary and ending concentration of cadmium metal ion, the cadmium volume, and the adsorbent mass, respectively.

The removal efficiency of Cd^{2+} by LDH-Cit/PVC was determined using E_q (2):

$$\text{Removal efficiency} = \left[\frac{(Ci - Cf)}{ci}\right] \times 100 \quad (2)$$

where C_i and C_f are the initial and final concentration of metal ions (mg L^{-1}), respectively.

3 Results and Discussion

In LDHs, as the interlayer anions are simply exchangeable, different kinds of anions can be intercalated in its structure. Intercalation of anionic ligands is also an efficient way to incorporate various metal cations to LDHs. The capacity of LDHs as adsorbents of pollutant has been extensively reported both for organic and inorganic anions. Finding an effective method to remove heavy cations such as Cd^{2+} from contaminated water depends on a selection of factors like cost, accessibility, and environmental health [25, 26]. Here, LDH-Cit/PVC NCs were prepared by mixing of CaFe/LDH-Cit with PVC solution via the solution intercalation process. First, bio-safe and organo-modified CaFe/LDH-Cit was prepared through the ultrasonic technique, and then LDH-Cit/PVC NCs were synthesized using the mixing of LDH suspension with PVC solution under desired conditions (Fig. 1).

3.1 FT-IR Study

The FT-IR spectra of CaFe/LDH-Cit, neat PVC and LDH-Cit/PVC NC are shown in Fig. 2. In the FT-IR spectrum of CaFe/LDH-Cit, the hydroxyl group stretching is verified by a peak at 3434 cm^{-1}. The presence of citrate anion determined by the formation of two absorption bands first appears at 1606 cm^{-1} related to asymmetrical vibration of CO_2^- and second at 1428 cm^{-1} is due to symmetrical vibration of CO_2^-. The citrate hydroxyl C-O group appears at 1080 cm^{-1}. M–O stretching and M–OH bending vibrations appeared at 625, 553 and 430 cm^{-1}. Neat PVC shows absorption bands at 2850–2950 cm^{-1} because of C–H stretching, the vibrating of methylene groups displayed at 1430 cm^{-1}, stretching of C–H in CHCl was exhibited at 1258 cm^{-1}. The characteristic bands at 614 and 695 cm^{-1} which are affiliated to the vibration stretching of C–Cl bonds of syndiotactic and isotactic structures of PVC similar to the literature [27]. There are both filler and polymer peaks in the FT-IR spectra of the NC films and with the increase in the amount of LDH-Cit in PVC matrix; absorption bands of the LDH were intensified [28]. With respect to the FT-IR spectra of the LDH-Cit/PVC NC, the presence of LDH-Cit in PVC matrix results in minor distinctions in the intensity of absorption bands, furthermore the adding of novel absorption bands is observed in the range 3300–3100 cm^{-1} accrediting to the vibrations of O–H groups for LDH-Cit which was loaded into the PVC matrix. Because of the low concentration of LDH-Cit in the polymer matrix, the later bands is not very clear in Fig. 2.

3.2 XRD Study

XRD is an important and convenient technique for identification of the crystal structure and the exfoliation and/or intercalation of the layered nanoparticle. XRD patterns of LDH and NCs containing 5 and 10 wt% of LDH-Cit is

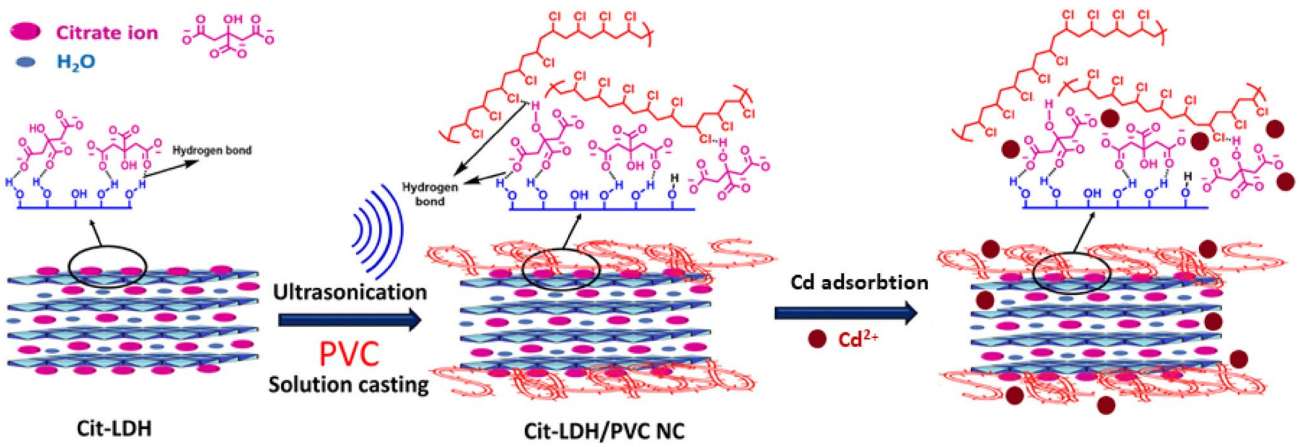

Fig. 1 Schematic illustration for the synthesis of LDH-Cit/PVC NC and adsorption of Cd^{2+} ions

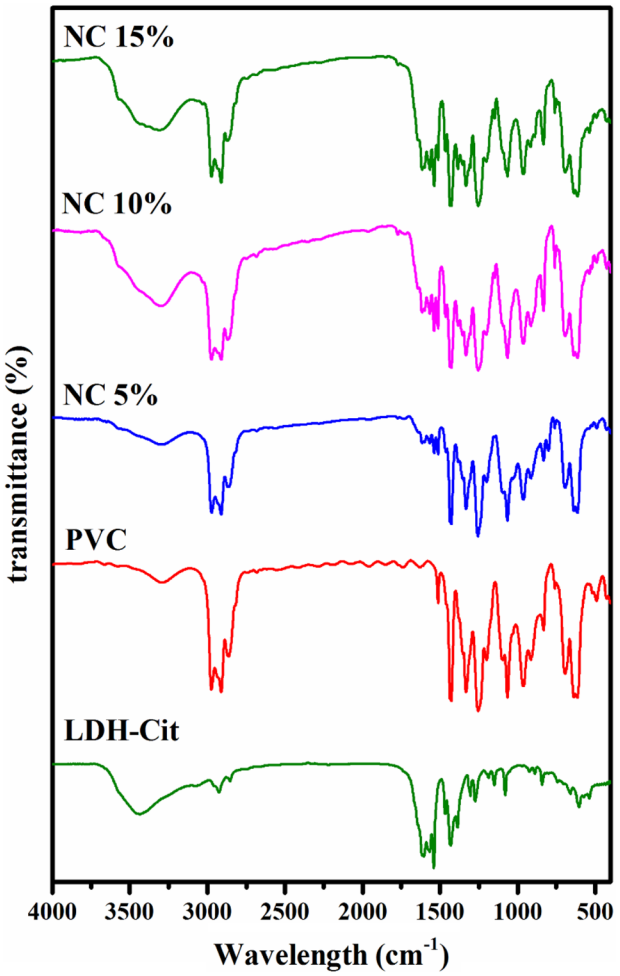

Fig. 2 FT-IR spectra of LDH-Cit, neat polymer, and LDH-Cit/PVC NCs

shown in Fig. 3. XRD pattern of LDH displayed the (0 0 3) diffraction at approximately 2θ = 10°. The presence of this reflection confirms the layered nature of the synthesized LDH. With respect to the Bragg's Law (Eq. 3), the interlayer d-value of LDH calculated 1.13 nm:

$$n\lambda = 2d \sin\theta \quad (3)$$

where d is the spacing between of crystal sheets and, also θ, n and λ are the angle in a common Bragg–Brentano geometry, reflection factor, and wavelength, respectively. XRD pattern of PVC showed amorphous reflection in high angle and it does not have any diffraction band in the 2θ region ranged from 1° to 10°. The XRD patterns of the LDH-Cit/PVC NC films with different concentration of the LDH nanoparticle were the same as pure PVC and the LDH-Cit's diffraction peaks were not observed. It is probably due to the fine dispersion and separated layers and the exfoliation state [28].

3.3 Thermal Properties

TGA is a heat dissipation method that examines the changes in the samples weight loss and also the sample heat destruction at various temperatures. The TGA curves of pure PVC and LDH-Cit/PVC NC with different amounts of the LDH-Cit nanoparticles are demonstrated in Fig. 4. Neat PVC shows a two-step degradation process. The first one consist of dehydrochlorination of PVC nearby 250–350 °C and another at 400–520 °C includes the breaking of the PVC backbone because of the loss or pyrolysis to low molecular mass fragments produced. The results show that the thermal stability of PVC is improved with the addition of LDH-Cit. Char yield can be used as a decisive coefficient for an estimated limiting oxygen index (LOI) of the polymers [29].

$$LOI = 17.5 + 0.4\,CR \quad (4)$$

where CR is char yield.

Results show that the char yield of PVC was increased from 8 to 23% by adding CaFe/LDH-Cit nanofiller to the polymer matrix. Also, the LOI values increased from 20 to around 26 in NC. According to the data [30], they can be put in self-extinguishing materials classification. This improvement in the char formation is attributed to the high heat resistance employed by the CaFe/LDH-Cit. In the second stage of degradation, the percentage of weight loss in NC was decreased may be due to the reduced breaking of PVC skeleton chains by adding LDH-Cit into the PVC matrix.

3.4 Morphological Studies (FE-SEM and TEM)

FE-SEM and TEM images of CaFe/LDH-Cit with different magnifications were shown in Fig. 5. Fe-SEM of CaFe/LDH-Cit powder showed dense particles with spherical morphology, porous surfaces, and layered structure. Figure 5 also displays the TEM images of the LDH-Cit. In the TEM images of this sample, it has observed that LDH-Cit has a clear nanostructure layers with uniform size distribution. The average diameter of the LDH layers is 13 nm.

The FE-SEM images of PVC NCs with different amount of CaFe/LDH-Cit (5, 10, and 15 wt%) shows that the surface morphology was changed in comparison to neat PVC (Fig. 6). A homogeneous incorporation of LDH-Cit in the polymer matrix was observed. Also, the EDX spectrum of the LDH-Cit/PVC and the presence of Ca, Fe, Cl, and C was displayed in Fig. 6g which has confirmed the incorporation of LDH in PVC matrix.

Another reason for the homogeneity of incorporation obtained from TEM analyses which are in a good correlation with XRD and FE-SEM data. In the TEM images of PVC containing 10 wt% of LDH (Fig. 7), the brighter region is related to PVC matrix and dark parts exhibited the

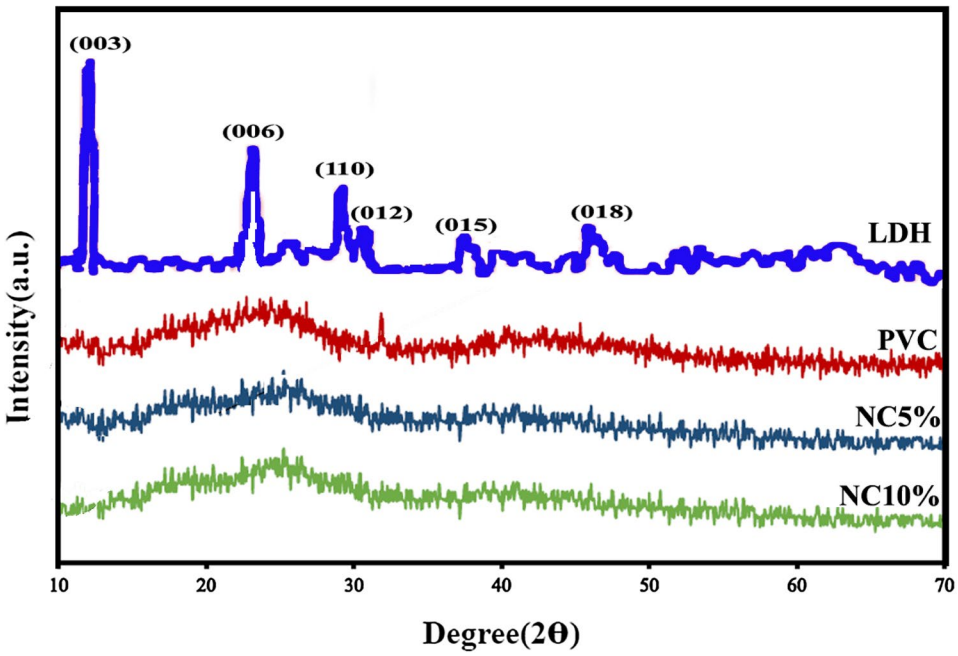

Fig. 3 XRD patterns of LDH-Cit, pure PVC, LDH-Cit/PVC NC 5 and 10 wt%

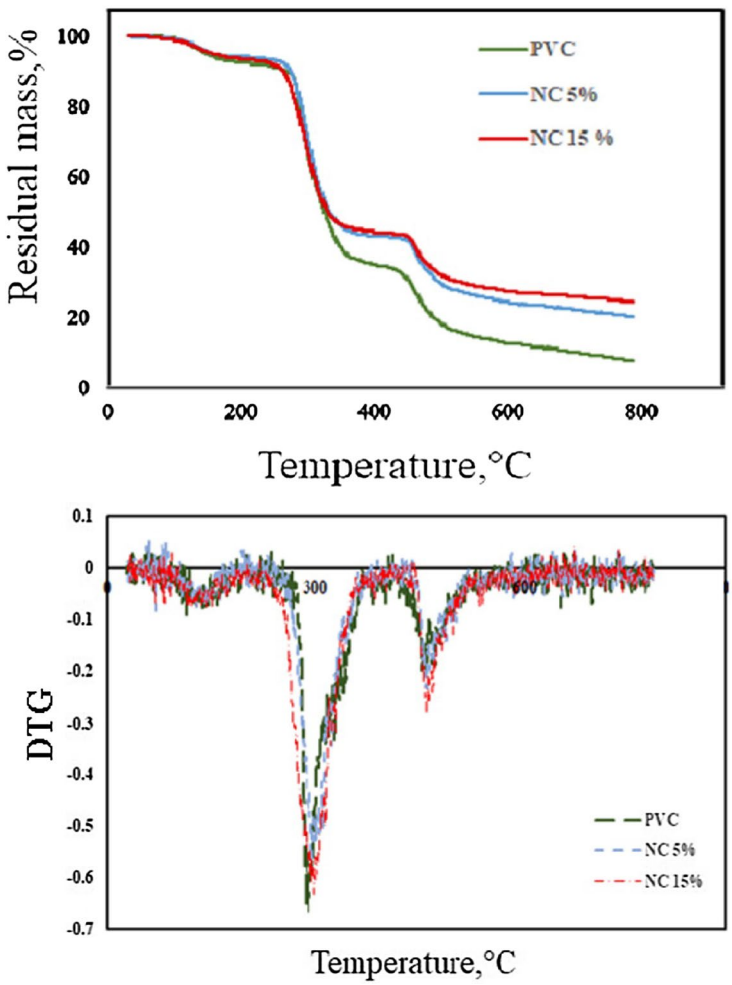

Fig. 4 TGA and DTG thermogram of neat PVC, NC 5 wt% and NC 10 wt%

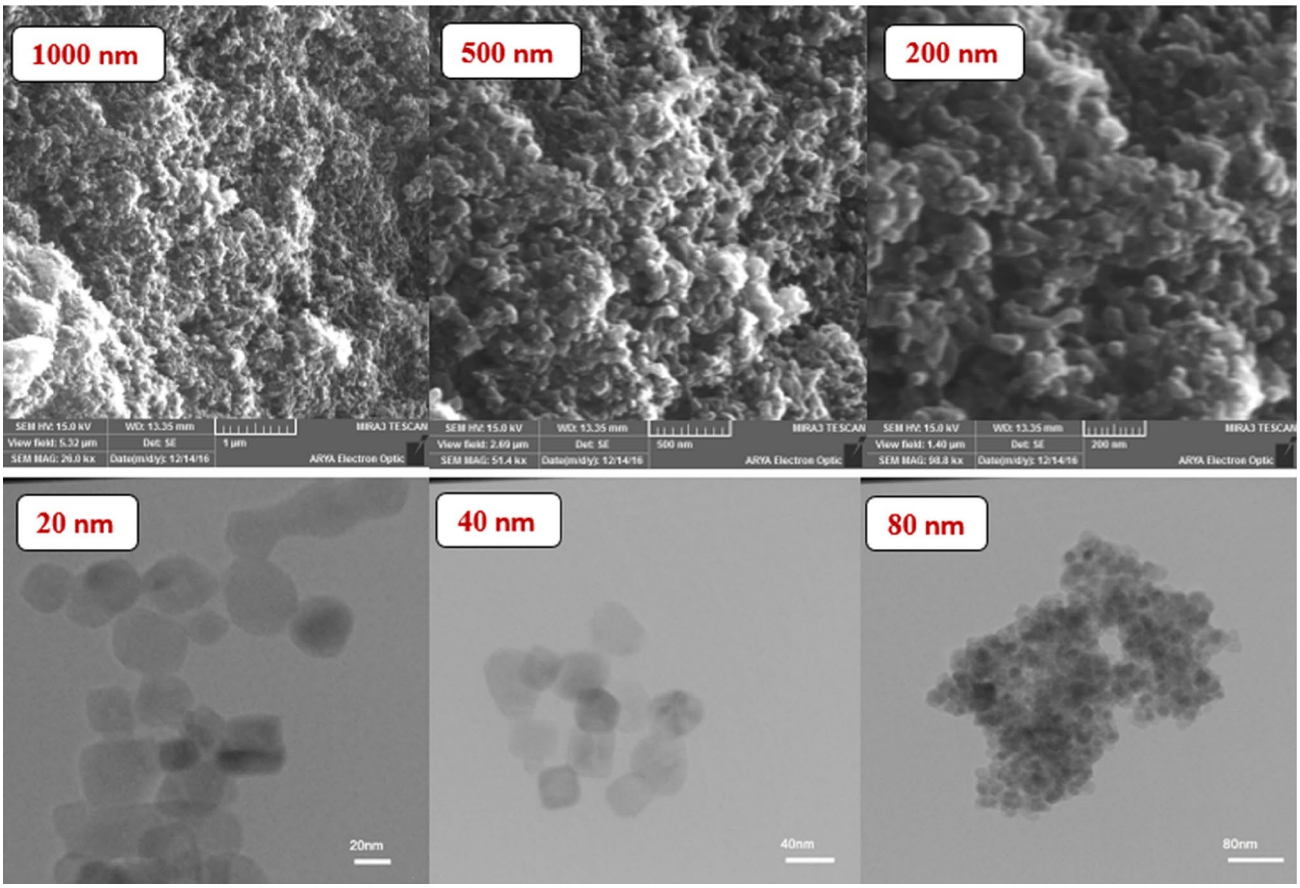

Fig. 5 FE-SEM photographs and TEM images of LDH-Cit with tree magnifications

LDH layers in the structure. Two types of LDH layers were observed in TEM images which are related to the agglomeration of and dispersion LDH layers. The darker sides are corresponding to poor delamination of LDH layers and the brighter sides are related to dispersing layers of LDH in the polymer matrix [31]. Although, exfoliation of LDH layers may cause intercalation of PVC chains into LDH layers which resulted in omitting low angles diffraction peaks of LDH with $2\theta = 0°–10°$.

3.5 Mechanical Properties

Figure 8 shows the mechanical properties of LDH-Cit/PVC NC at different contents of LDH and the results are summarized in Table 1. Results show that the overall mechanical properties of LDH-Cit/PVC NC are significantly improved compared to the pure PVC sample. By increasing the content of modified LDH into PVC, the tensile strength and elongation at F_{ax} for NC are improved due to the interaction between the modified LDH and PVC chain. This can shift the pressure from the PVC matrix to fillers and considerable progress was seen in the mechanical properties [32–34].

3.6 Adsorption Study

The adsorption behavior of NCs and pure polymer for the removal of Cd^{2+} ions from aqueous solution was investigated by performing batch adsorption experiments.

3.6.1 The Effect of pH

To figure out the effect of pH on the adsorption capacity, 10 mL of the 10 mg L^{-1} cadmium was prepared in universal-buffer prepared in deionized water. Figure 9 describes how the pH effects the adsorption of Cd^{2+} onto LDH-Cit/PVC NC 10 wt% in the range of 2–11, that these amounts were attending by adding 1 M sodium hydroxide or diluted HCl, just in case of maintaining other experimental parameters constant. As soon as the pH increases, the metal removal will be raised. The adsorption values of Cd^{2+} was increasing by pH to 7 at room temperature. Due to the experiments that have been undertaken for Cd^{2+} adsorption, lower adsorption efficiency is because of an excessive protonation of the lone pair of electrons on oxygen of functional groups, ends up with repellent vigor between the adsorbate and adsorbents [35].

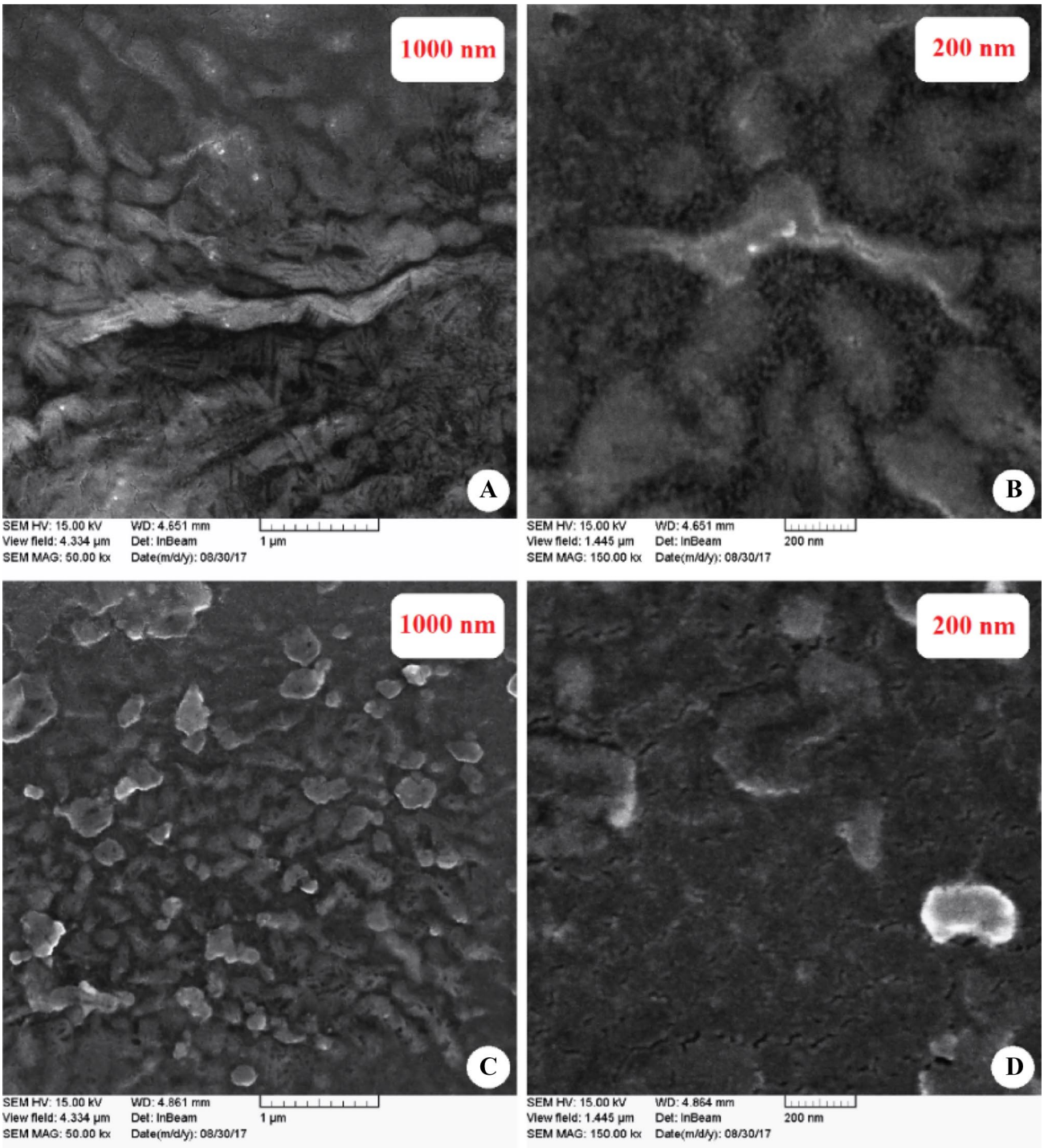

Fig. 6 FE-SEM photographs of LDH-Cit/PVC NC 5 wt% (**a**, **b**), NC 10 wt% (**c**, **d**) and NC 15 wt% (**e**, **f**) at different magnifications and EDAX of NC 5 wt% (**g**)

3.6.2 Effect of Contact Time

various adsorbents were added to 10 mg L^{-1} of cadmium solutions at 25 °C and then they were shake for different times (5, 10, 20, 40, 60, 80, 100, 120, 160, 180 and 200 min) to check the change of adsorption against time. The obtained results show that the removal capacity of cadmium was increased by increasing the contact time. Also, the rate of adsorption is increased to a constant

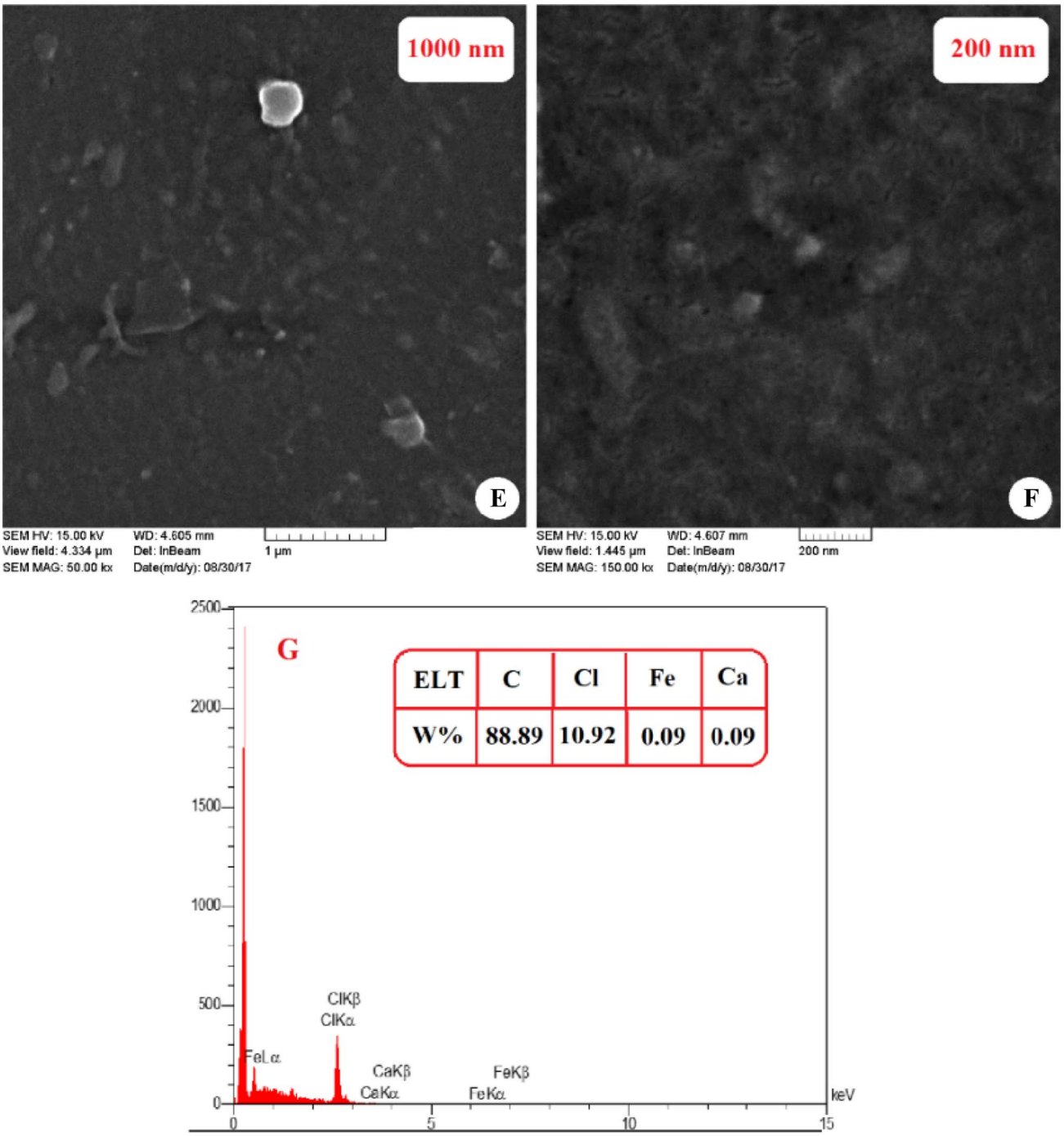

Fig. 6 (continued)

value after 120 min which reveals the equilibrium state of adsorption, similarly (Fig. 10).

3.6.3 Adsorption Kinetic

The kinetic models were brought to the proof that the adsorption behaviors of adsorbents samples in four models; pseudo-first order (Eq. 5), pseudo-second-order (Eq. 6), intra-particle diffusion (Eq. 7) and Elovich (Eq. 8) were studied [36].

$$\ln\left(q_{e,exp.} - q_t\right) = \ln q_{e,theory} - k_{1t} \tag{5}$$

$$t/q_t = 1/k_2 q_e^2 + t/q_e \tag{6}$$

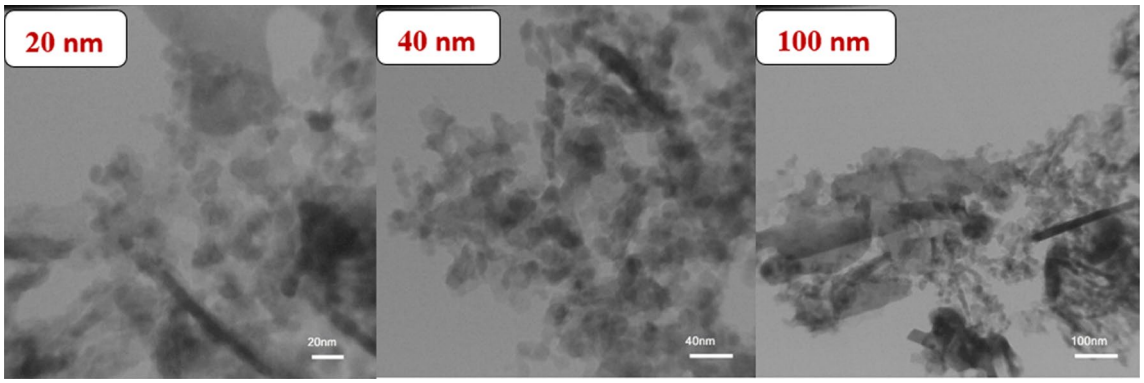

Fig. 7 TEM images of NC 15 wt%

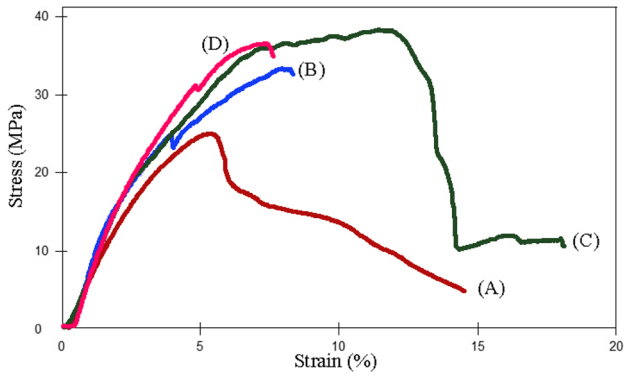

Fig. 8 Stress-strain diagrams of **a** pure PVC and **b–d** related NC with different contents

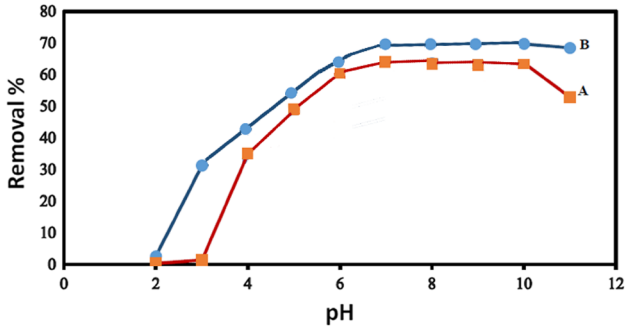

Fig. 9 Effect of pH on adsorption of Cd^{2+} ion; **a** neat PVC and **b** NC 10

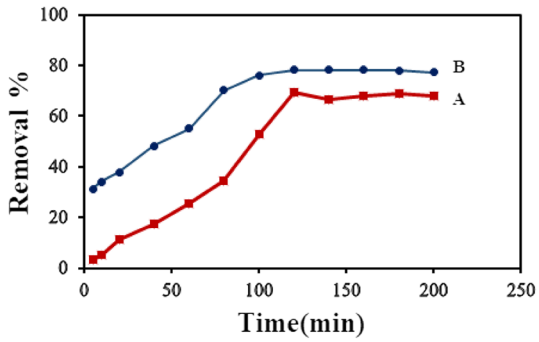

Fig. 10 Effect of contact time on adsorption of Cd^{2+} ions **a** PVC and **b** NC10%; (10 mL of cadmium cation solution, 10 mg of LDH, 298 K, pH 10)

Table 1 Mechanical properties of neat PVC and LDH-Cit/PVC NC

Sample	Strain (%)	Tensile strength (MPa)	Elongation (mm)
Pure PVC	25.18	5.15	1.54
NC5%	22.13	7.68	2.31
NC10%	35.33	13.35	4.01
NC15%	30.89	7.27	2.18

$$q_t = k_i t^{0/5} + C_i \quad (7)$$

$$q_t = \left(\ln\left(h_b\right) + \ln t\right)/B \quad (8)$$

where q_e, shows the Cd(II) adsorption capacity and q_t is the amount of Cd(II) adsorbed at the time. k_1 (min^{-1}), k_2 (g mg^{-1} min) and k_i (mg g^{-1} min) are kinetic constants related to the pseudo-first-order model, rate constant related to the second-order model, and a constant related to the intraparticle diffusion model, respectively. C_i can be calculated according to the intraparticle diffusion model, h_b and B are the Elovich constants and K_{intra} (mg g^{-1} $min^{-1/2}$) is the intraparticle diffusion rate factor. According to Fig. 11a (Elovich), 11b (intraparticle diffusion model), 11c (pseudo-second-order model) and 11d (pseudo-first order model) the linear plots were achieved. Table 2 reveals the adsorption kinetics parameter which is obtained from linear plots. The correlation coefficients (R^2) displayed that the

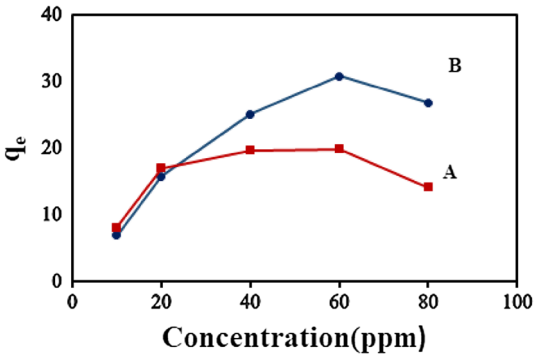

Fig. 11 Effect of concentration on adsorption of Cd^{2+} ions of **a** PVC and **b** NC10%

pseudo-second-order equation adjusted better ($R^2 = 0.9871$) than the pseudo-first-order equation ($R^2 = 0.8665$), Elovich ($R^2 = 0.771129$) and interparticle diffusion ($R^2 = 0.9219$) and also in pseudo-second-order equation comparison between experimental and theoretical Q_e, curve best fitted with the experimental data. Therefore, regarding the pseudo-second-order model, it can be estimated that chemical sorption has done.

3.6.4 Effect of Concentration

The effect of adsorbate concentration on Cd^{2+} adsorption was investigated by addition of optimal amount of adsorbent (0.10 g) to different adsorbate solutions (10, 20, 40, 60 and 80 mg L^{-1}) and shake them for 2 h at 25 °C. Then the adsorbent was centrifuged and the residue of Cd^{2+} was evaluated by FAAS, Eq (1) was used to calculate the amount of cadmium adsorbed. Figure 11 depicts the different amounts of Q_e with C_e for adsorbent samples. Removal percentage of Cd^{2+} was increased by increasing the Cd^{2+} concentration to 60 mg L^{-1}, for upper concentrations the removal content was not changed, which can be related to saturation of active sites of adsorbent samples at a higher concentration of Cd^{2+}.

3.6.5 Adsorption Isotherm

To investigate the adsorption behavior for cadmium ions, the equilibrium adsorption data are estimated by Langmuir (Eq. 8) and Freundlich isotherms(Eq. 9), Elovich (Eq. 10) and interparticle diffusion (Eq. 11) kinetics models are shown in equations [37].

$$Ce/Q_e = 1/bQ_m + Ce/Q_m \tag{8}$$

$$Ln/Q_e = \ln\ K_f + 1/n\ \ln C_e \tag{9}$$

$$q_t = (\ln(hb) + \ln t)/B \tag{10}$$

$$q_t = \mathrm{Kintrat}_{1/2} + C \tag{11}$$

where C_e (mg L^{-1}) and Q_e (mg g^{-1}) are the equilibrium concentration of cadmium and the equilibrium absorption capacity, respectively. Q_m (mg g^{-1}) is the maximum adsorption capacity, and the Langmuir constant is named b (L mg^{-1}). K_f and n are Freundlich constants are linked with adsorption capacity and the adsorption intensity, h_b and B are the Elovich constants and Kintra (mg g^{-1} $min^{-1/2}$) is interparticle diffusion constants and *t* (min) is the adsorption time (Fig. 12). In addition, by using the Langmuir equation, it can be proved that the system of absorption is desirable or undesirable. This feature is determined by the help of a non-dimensional constant called the separation factor or equilibrium parameter (R_L). The R_L expresses the tendency to formation superficial complex. Whatever the K_L getting more this tendency is getting greater. If $R_L = 0$ is the irreversible absorption system, and if $R_L = 1$ is an undesirable absorption system and $0 < R_L < 1$ absorption is desirable and there is no interaction between the adsorption molecules. R_L is based on the equation shown below in (Eq. 12) [38]:

$$R_L = 1/\left(1 + bC_0\right) \tag{12}$$

where b is the Langmuir constant and C_0 is the initial Cd(II) concentration (mg L^{-1}).

Table 3 explains obtain parameters from two models at room temperature. Due to results, we can understand that the Langmuir model is the most suitable isotherm for

Table 2 Kinetic parameters for the adsorption of Cd^{2+} through different adsorbent samples

Samples	Pseudo-first order			Pseudo-second order	
	K1 (min^{-1})	R^2	q_e	K^2 (min^{-1})	R^2
PVC	3.2918	0.918	23	1852.831	0.5382
NC10%	2.703	0.8665	25	16.25508	0.9871

Samples	Elovich			Intraparticle diffusion		
	B	h_b	R^2	k_i	C_i (mg g^{-1} $min^{-1/2}$)	R^2
PVC	0.154368	0.0000011	0.8648	2.0048	−4.9057	0.9409
NC10%	0.216892	0.771129	0.9231	1.3671	6.4942	0.9219

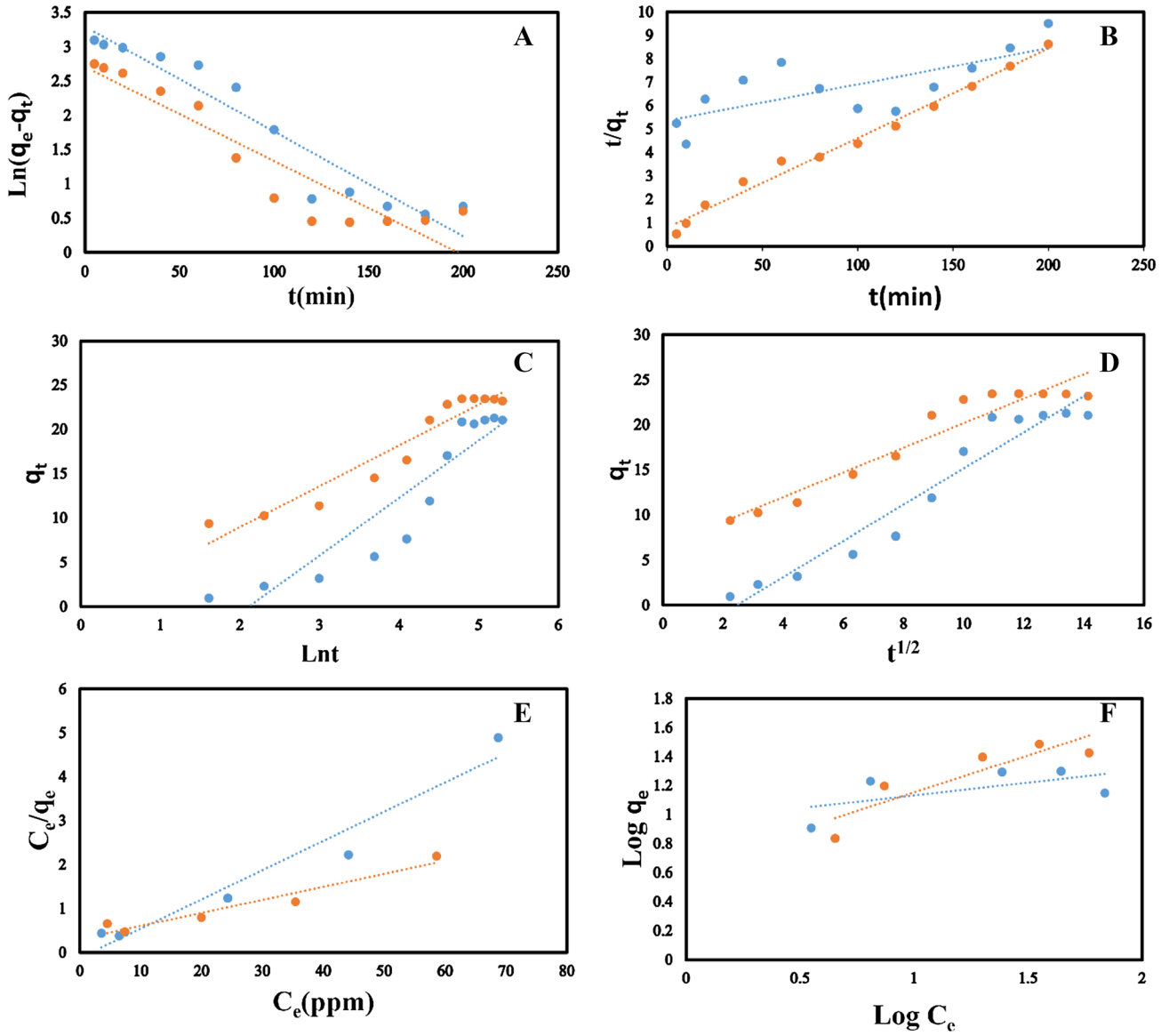

Fig. 12 **a** Pseudo-first-order kinetic model, **b** pseudo-second-order kinetic model, **c** Elivich kinetic model, **d** interparticle diffusion kinetic mode, **e** Langmuir isotherm, and **f** Freundlich isotherm

Table 3 Langmuir and Freundlich isotherms adsorption parameters of cadmium on different samples (T = 25 °C and sorbent dosage = 10 mg)

Sample	T (K)	Langmuir constants			Freundlich constants		
		q_m (mg g^{-1})	k_l	R^2	kf	n	R^2
PVC	273	− 0.06226	− 20.8652	0.9483	6.510394	0.116322	0.3583
NC10%	273	− 0.8547	− 9.53545	0.9337	− 2.05,855	0.198181	0.797

adsorption of cadmium metal ion for NC10% ($R^2 = 0.9337$). These results shed light on the interactions among the adsorbent and adsorbate materials have a monolayer adsorption mechanism. Furthermore, the R_L amounts for the LDH-Cit/PVC 10 wt% NC adsorbents are desirable (in the range of $0 < R_L < 1$). Surprisingly the increase in the maximum adsorption capacities of Cd^{2+} for LDH-Cit/PVC 10 wt% NC is obviously greater than the neat PVC at ambient temperature. More ever, according to Table 3, LDH-Cit/PVC can be a good choice as a desirable absorbent for the removal of cadmium from wastewaters owing to the hydroxyl groups of LDHs. Totally LDH-Cit/PVC NC has synthesized with

the ultrasonic method as a green and low-cost method and also is constable owing to the very small amount of sorbent (0.10 g) for the removal of cadmium from aqueous solution. More importantly, the rate of adsorption is favorable (120 min), and it is noticeable that there is a low percentage of LDH in the NCs.

4 Conclusions

In summary, organo-modified CaFe/LDH with citrate anion was effectively prepared by the homogenous co-precipitation method. Then LDH-Cit/PVC NC films with the different amount (5, 10 and 15 wt%) of citrate-modified LDH nanoparticles were synthesized by ultrasonic irradiation techniques. Citrate anion was used as a coupling agent to increase compatibility between the PVC matrix and inorganic. Homogenous and uniform dispersity forms of NC with a high degree of intercalation and partially LDH exfoliation demonstrated by FE-SEM and TEM images. The thermal properties of the PVC were enhanced by adding LDH-Cit to the matrix. Moreover, the tensile properties of NCs were enhanced. Also LDH-Cit/PVC NCs performance in cadmium removal from the aqueous solution was investigated and the received data demonstrated the great removal capacity of the LDH-Cit/PVC NCs for elimination and up taking toxic Cd^{2+} ion in compared to PVC from aqueous solution. These results offer a green solution to multiple problems, including the removal of heavy metal ions from wastewater and also LDH-Cit could be a promising class of thermal stabilizer for PVC with non-toxicity, environmentally-friendly, and economical features.

Acknowledgements This work was supported partially by the Research Affairs Division of Isfahan University of Technology.

Compliance with Ethical Standards

Conflict of interest The authors stated that there are no conflicts of interest in this work.

References

1. M. Arshadi, H. Eskandarloo, M.K. Abdolmaleki, A. Karimi Abbaspourrad, ACS Sustain. Chem. Eng. **6**(10), 13332–13348 (2018)
2. H. Lu, Q. Li, H. Xiao, R. Wang, D. Xie, Am. J. Anal. Chem. **5**, 547 (2014)
3. F. Yang, S. Sun, X. Chen, Y. Chang, F. Zha, Z. Lei, Appl. Clay Sci. **123**, 134–140 (2016)
4. J. Yin, T. Wu, J. Song, Q. Zhang, S. Liu, R. Xu, H. Duan, Chem. Mater. **23**, 4756–4764 (2011)
5. S. Duan, W. Ma, Z. Cheng, P. Zong, X. Sha, F. Meng, Colloids Surf. A **490**, 250–257 (2016)
6. F. Fu, Q. Wang, J. Environ. Manag. **92**, 407–418 (2011)
7. S.S. Gupta, K.G. Bhattacharyya, Adv. Colloids Interface Sci. **162**, 39–58 (2011)
8. A. Saeed, M. Iqbal, M.W. Akhtar, J. Hazard. Mater. **117**, 65–73 (2005)
9. A.S.K. Kumar, S. Kalidhasan, V. Rajesh, N. Rajesh, Ind. Eng. Chem. Res. **51**, 58–69 (2011)
10. M. Dinari, P. Asadi, S. Khajeh, New J. Chem. **39**, 8195–8203 (2015)
11. E.P. Giannelis, Adv. Mater. **8**, 29–35 (1996)
12. I. Khelifa, A. Belmokhtar, R. Berenguer, A. Benyoucef, E. Morallon, J. Mol. Struct. **1178**, 327–332 (2018)
13. A. Belalia, A. Zehhaf, A. Benyoucef, Polym. Sci. Ser. B **60**, 816–824 (2018)
14. B.K. Deka, T.K. Maji, M. Mandal, Polym. Bull. **67**, 1875–1892 (2011)
15. V.K. Thakur, R.K. Gupta, Chem. Rev. **116**, 4260–4317 (2016)
16. T. Tongesayi, J. Kugara, S. Tongesayi, Environ. Geochem. Health **40**, 375–381 (2018)
17. S. Daikh, F. Zeggai, A. Bellil, A. Benyoucef, J. Phys. Chem. Solids **121**, 78–84 (2018)
18. W.T. Reichle, Solid State Ionics **22**, 135–141 (1986)
19. D. G. Evans, R. C. Slade, in *Layered Double Hydroxides* (Springer, Berlin, 2006), pp. 1–87
20. K. Yamani, R. Berenguer, A. Benyoucef, E. Morallón, J. Therm. Anal. Calorim. **135**, 2089–2100 (2019)
21. F. Leroux, J.-P. Besse, Chem. Mater. **13**, 3507–3515 (2001)
22. S.T. Liu, P.P. Zhang, K.K. Yan, Y.H. Zhang, Y. Ye, X.G. Chen, J. Appl. Polym. Sci. **132**, 42524 (2015)
23. F.J. Labuschagne, D.M. Molefe, W.W. Focke, I. Van der Westhuizen, H.C. Wright, M.D. Royeppen, Polym. Degrad. Stab. **113**, 46–54 (2015)
24. O. Rahmanian, M. Dinari, S. Neamati, Environ. Sci. Pollut. Res. **25**, 36267–36277 (2018)
25. G. Tan, Z. Li, H. Yuan, D. Xiao, Sep. Sci. Technol. **49**, 1566–1573 (2014)
26. D. Van Krevelen, Polymer **16**, 615–620 (1975)
27. S.K. Mahto, S. Das, A. Ranjan, S.K. Singh, P. Roy, N. Misra, RSC Adv. **5**, 45231–45238 (2015)
28. Y.-Z. Bao, Z.-M. Huang, Z.-X. Weng, J. Appl. Polym. Sci. **102**, 1471–1477 (2006)
29. S. Mallakpour, M. Hatami, Appl. Clay Sci. **149**, 28–40 (2017)
30. S. Mallakpour, M. Dinari, J. Inorg. Organomet. Polym. Mater. **22**, 929–937 (2012)
31. Y. Kuroda, Y. Miyamoto, M. Hibino, K. Yamaguchi, N. Mizuno, Chem. Mater. **25**, 2291–2296 (2013)
32. Y. Li, S. Wu, L. Pang, Q. Liu, Z. Wang, A. Zhang, Constr. Build. Mater. **172**, 584–596 (2018)
33. S. Mallakpour, R. Aalizadeh, Synth. React. Inorg. Met. Org. NanoMet. Chem. **44**, 1450–1456 (2014)
34. C. Liu, Y. Luo, Z. Jia, B. Zhong, S. Li, B. Guo, D. Jia, Express Polym. Lett. **5**(7), 591–603 (2011)
35. M. Dinari, R. Tabatabaeian, Carbohydr. Polym. **192**, 317–326 (2018)
36. V. Devi, M. Selvaraj, P. Selvam, A.A. Kumar, S. Sankar, K. Dinakaran, J. Environ. Chem. Eng. **5**, 4539–4546 (2017)
37. G. Mohammadnezhad, R. Soltani, S. Abad, M. Dinari, J. Appl. Polym. Sci. **134**, 45383 (2017)
38. Z. Hu, G. Chen, J. Mater. Chem. A **2**, 13593–13601 (2014)